

Available online at [www.sciencedirect.com](http://www.sciencedirect.com)**ScienceDirect**

Physics Procedia 83 (2016) 1261 – 1270

Physics

**Procedia**9<sup>th</sup> International Conference on Photonic Technologies - LANE 2016

## IR-thermography for quality prediction in selective laser deburring

Mauritz Möller<sup>a,\*</sup>, Christian Conrad<sup>a</sup>, Walter Haimerl<sup>b</sup>, Claus Emmelmann<sup>a</sup><sup>a</sup>*Institut of Laser and System Technologies (iLAS), Hamburg University of Technology (TUHH), Denickestr. 17, 21073 Hamburg, Germany*<sup>b</sup>*HAIMERL Lasertechnik GmbH, Mühlstrasse 41, 71229 Leonberg*

---

### Abstract

Selective Laser Deburring (SLD) is an innovative edge-refinement process being developed at the Laser Zentrum Nord (LZN) in Hamburg. It offers a wear-free processing of defined radii and bevels at the edges as well as the possibility to deburr several materials with the same laser source.

Sheet metal parts of various applications need to be post-processed to remove sharp edges and burrs remaining from the initial production process. Thus, SLD will provide an extended degree of automation for the next generation of manufacturing facilities.

This paper investigates the dependence between the deburring result and the temperature field in- and post-process. In order to achieve this, the surface temperature near to the deburred edge is monitored with IR-thermography. Different strategies are discussed for the approach using the IR-information as a quality assurance. Additional experiments are performed to rate the accuracy of the quality prediction method in different deburring applications.

© 2016 The Authors. Published by Elsevier B.V. This is an open access article under the CC BY-NC-ND license

(<http://creativecommons.org/licenses/by-nc-nd/4.0/>).

Peer-review under responsibility of the Bayerisches Laserzentrum GmbH

**Keywords:** laser cutting; selective laser deburring; IR-thermography; quality assurance

---

### 1. Introduction

To fulfil today's quality standards, laser cut sheet metal parts often need to be post-processed. Similar to many other manufacturing processes, edge refinement is an important production step. Burrs have a bad influence on practicality, safety and aesthetics (Schäfer und Breuninger 1975). Especially the removal of burrs takes a high percentage of today's production costs and time (Beier und Nothnagel 2015; Gillespie 2007; Beier 1999). Up to 9 % of the production costs are caused by deburring different materials in different applications. Only in Germany the

---

\* Corresponding author. Tel.: +49-176-1484-0130 .

E-mail address: [mauritz.moeller@lzn-hamburg.de](mailto:mauritz.moeller@lzn-hamburg.de)

costs produced by burrs are estimated to 500 million Euro, including deburring, higher manpower, cycle times, or machine breakdowns for example (Aurich et al. 2009). A universal solution for the edge refinement does not exist although there are plenty of deburring processes.

The deburring with laser radiation has already been investigated. Lee et al. (2000) showed that laser deburring offers flattering features compared to the existing deburring systems. The HAZ can be reduced to a minimum, even precision components can be deburred and an automated deburring is possible. Through different heat contributions the laser deburring process fundamentally changes. Burrs can be remelted, cutted, sublimated and oxidized with laser radiation (Schmidt-Sandte 2002). SLD is a laser deburring process in which the edges and burrs are remelted to defined radii. Moveable mirrors grant fast processing and one laser source is able to deburr different materials wear-free.

This paper investigates if IR-thermography is a suitable technology to assure quality of laser deburred edges. The main characteristic of SLD remelted is the radius of the round edge. Different settings of factors such as for example the laser power or the number of exposures affect this radius. One aim of the quality assurance is to guarantee a constant radius at every edge. During the SLD development the positioning of the laser spot towards the edge had an obvious effect on the deburring result. Based on this finding, this paper tries to find a link between the edge temperature and the position of the laser spot. A quality assurance should also detect flaws. Mechanical and chemical flaws are observed in this paper.

## 2. State of the art

The edge geometry is evaluated to review the quality of the deburred edges. There are many edge measurement systems available to detect remaining burrs (Beier 1999). These measuring methods differ in their measuring dimensions, the contact to the sample, the possibility to measure in-process and the destructive or non-destructive measurement (Aurich et al. 2009). Usually, a single and essential measure of the edge is determined to classify the deburring quality and simultaneously cut measuring costs (Thilow 2008). Occurring edges in SLD stand out due to different achieved radii. For this reason the rounding  $r$  is considered as a measure to qualify the deburring results.

As shown by Schmidt-Sandte (Schmidt-Sandte 2002), the achieved surface temperature during SLD has a link to the important and adjustable factors involved, like in equation 1. This includes factors like the laser power, the focus diameter, the speed and the number of exposures. This leads to the assumption that the edge quality described by the achieved radii has a direct link to the edge temperature.

$$T(0, t)_{\text{Gauss}} = A \cdot I_0 \frac{d_f}{2\lambda\sqrt{2\pi}} \cdot \arctan\left(\frac{4\sqrt{2\kappa t}}{d_f}\right) \quad (1)$$

IR-thermography has some advantages in comparison to other measurement technologies. The measurement provides thermal images in real time, without contact to the measured surface and without destruction of the surface (Bernhard 2014; Bagavathiappan et al. 2013). IR-thermography has already been examined for many other applications and their temperature field. A large number of applications has been discussed in literature (Usamentiaga et al. 2014; Bagavathiappan et al. 2013). Thermography has already been used to find and locate cracks and flaws in steel and stainless steel components (Barile et al. 2016; Schausberger et al. 2015). Particular laser processes can be examined with ir-thermography (Purtonen et al. 2014). It has already been demonstrated that ir-thermography is a powerful tool to monitor the quality of laser welded polymers (Speka et al. 2008). Krauss et al. showed that ir-thermography is a suitable tool to control a selective laser melting process (Krauss et al. 2014). Furthermore, the welding of metallic materials and its on-line monitoring for quality issues is possible (Bagavathiappan et al. 2013; Spellenberg et al.). In the following, ir-thermography is tested for a quality assurance in SLD processes.

### 3. Setup

#### 3.1. Material and edge condition

The experiments are carried out with samples out of the stainless steel 1.4301. Apart from the laser cutting process the samples do not undergo another treatment. In all experiments, the upper edge of the sheet metal parts is used.

#### 3.2. Burr geometry after laser cutting and deburring result

Laser cut stainless steel sheets with a thickness up to 4 mm show high cutting quality. Generally, the burrs are located non-periodically and randomly along the cut geometry. Typical edge cross sections after laser cutting and laser deburring are illustrated in Fig. 1.

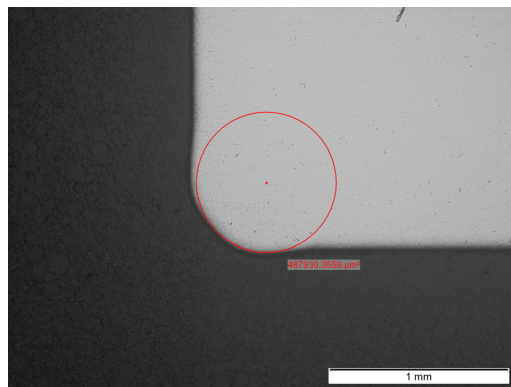


Fig. 1. Optimal edge condition after SLD.

The edge condition after the SLD process is dependent on many influence factors in the manufacturing process. The mean curvature radii for the deburred edges are illustrated in Fig. 2.

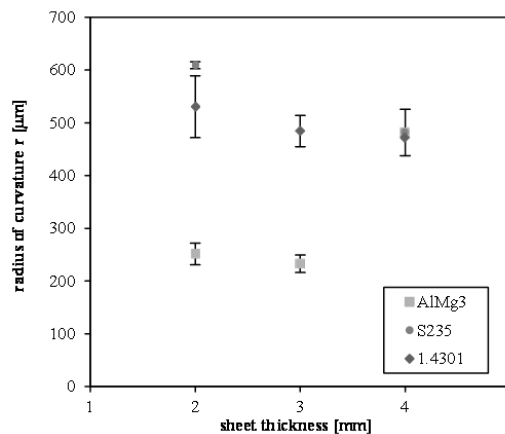


Fig. 2. Mean curvature radii for different materials and sheet thicknesses after SLD.

### 3.3. Experimental setup

The investigations are executed with a Trumpf TruDisk 5001 multi-mode continuous wave disk laser with a laser power of 5 kW at a wavelength of  $1.03\ \mu\text{m}$ . The scanning optic Trumpf PFO 3D is used to enable a laser remote process under surrounding atmosphere and an angle of  $45/135$  degree between the top of the sample and the laserbeam (Fig. 3).

The infrared camera is an IRCam Equus 81kM MCT. This camera system works at a spectral range of  $3\text{--}5\ \mu\text{m}$  and with a resolution of 256 rows and 320 columns. In the given setup the camera depicts a surface of  $9,79\ \text{mm} \times 12,24\ \text{mm}$ . The infrared camera is installed with an angle of  $90$  degrees towards the surface of the samples. To increase the resolution a spacer is installed between the objective and the camera. Moving the objective  $70\ \text{mm}$  away from the camera enables a lower working distance.

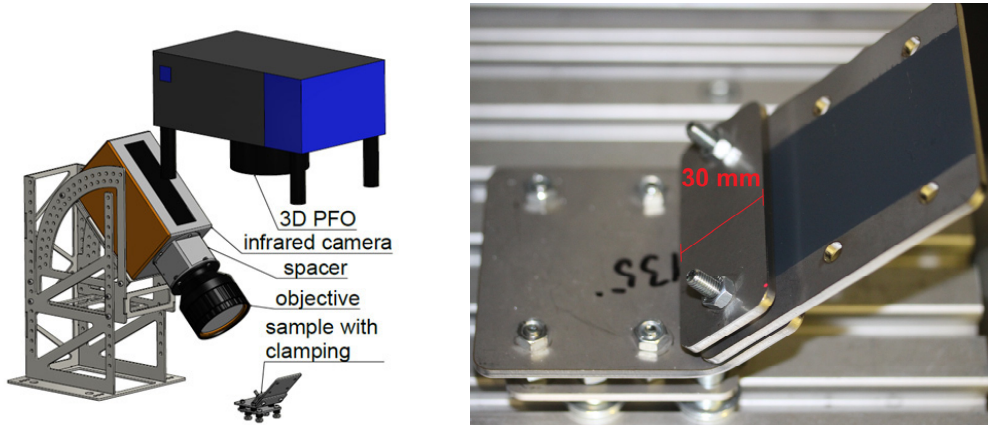


Fig. 3. (a) Experimental set-up, (b) specimen clamping set-up.

A calibration is needed to conclude from the measured intensity to the corresponding temperature. To exclude as many sources of errors as possible, the calibration is executed in the same setup as the investigations. During a constant warming of a calibration sample, the surface temperature is recorded with a thermocouple type K. A maximal surface temperature of  $500$  degree Celsius is measured.

### 3.4. Method

Figure 4 (a) shows the measured infrared radiation in the camera unity ‘counts’ during the SLD process. To match the different recordings  $0\ \text{s}$  describes the point in time when the laser spot is nearest to the middle of the picture at row 160. All following analysis times are referred to this point in time.

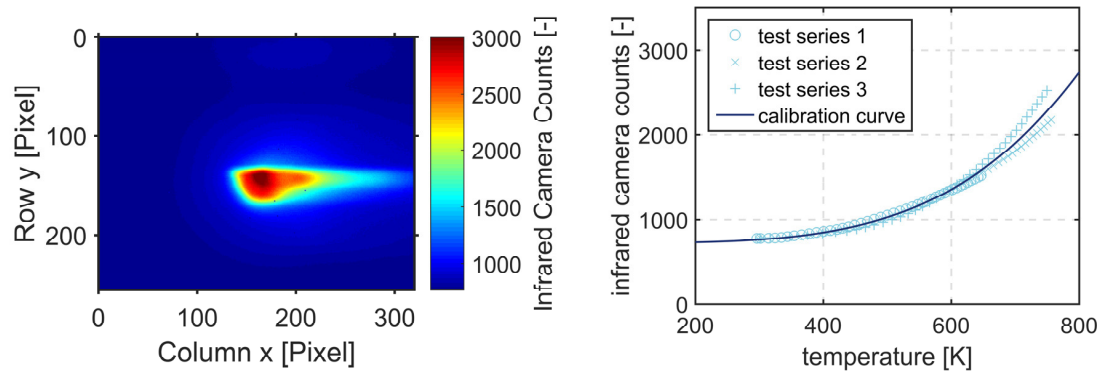


Fig. 4. (a) Measured IR-radiation ; (b) Calibration curves (camera counts vs. thermocouple measurement).

The relationship between the measured counts  $C$  and the corresponding surface temperature  $T$  in degree Celsius is described by a modified Stefan Boltzmann equation:

$$C(T) = a \cdot (T + 273,15K)^4 + b$$

The two fitting parameters  $a$  and  $b$  are needed to fit the calibration curve to the measured surface temperature during the calibration process. The parameters could be found to  $a = 4,924e-09$ ,  $b = 719,7$  and the calibration curve is shown in Fig. 4 (b).

Besides a calculation of the maximum measured temperature and a calculation of an arithmetic mean over a defined field next to the edge, there is another approach used to evaluate the measured temperatures. Depending on the investigated effect, different parts of the edge are examined. The arithmetic mean is calculated over a varying interval of rows for every column. The result is a temperature signature parallel to the exposure.

$$M(x, y) = 1/m \cdot \sum_{i=1}^m M(x, n-1+m)$$

$M$  is the matrix of the measured counts at a certain time extracted from the thermal images.  $n$  equates the first row and  $m$  equates the number of the including rows of the interval. For every column  $x$  the arithmetic mean is calculated over the defined row  $y$  interval. In the next step, the arithmetic mean over the executed repetitions is calculated so that finally the temperature signature parallel to the edge and among the defined row interval includes at least four repetitions. In case of the mechanical flaw evaluation the calculated temperature signature is edited by a non-parametric smoothing regression with a quadratic polynomial. Each smoothed value is determined by neighboring data points defined within the span of 10 % of the given data points.

## 4. Results and discussion

### 4.1. Correlation between achieved radii and edge temperatures

Figure 5 shows the measured radii across the measured temperatures in a test series with 25 different settings of parameters. The temperatures are determined during the laser exposure at a time of  $t = 0$  s and 0,25 s later. Both the evaluation of the maximum measured temperature and the evaluation of the temperature next to the edge show that there is a direct link between achieved radii and the temperature (Fig. 5).

Table 1. Process parameters for experiments.

Laser power [Watt]	Focus diameter [mm]	Speed [mm/s]	Number of exposures [-]
1000 - 3000	1,6 – 2,55	400 - 600	1 - 5

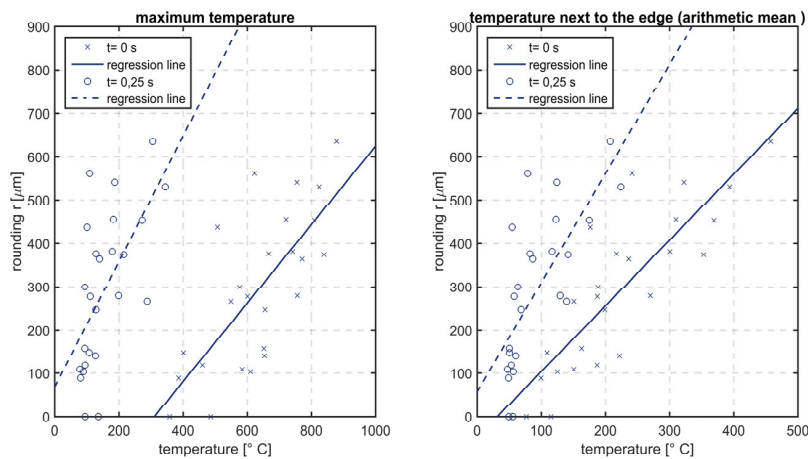


Fig. 5. (a) Maximum temperature on the specimen; (b) Mean temperature next to the edge.

### 4.2. Link between spot position and edge temperature

A test series with five positions was executed to investigate the influence of the laser spot position. Position 1 starts with a distance of 0,2 mm between laser spot midpoint and the edge. With every following position the laser spot is moved by 0,1 mm towards the edge so that in position 3 the laserspot is centred at the edge. The deburring parameters are listed in table 2. Every position is carried out four times. The thermal pictures are being evaluated at  $t = 0$  s and  $t = 0,1$  s. The evaluated surface has a range of 5 pixels which matches to 0,192 mm and is located at  $n = 95$  at the end of the remelted surface.

Table 2. Process parameters for spot position experiments.

Laser power [Watt]	Focus diameter [mm]	Speed [mm/s]	Number of exposures [-]
3000	2,05	400	1

Figure 6 shows the calculated temperature signatures for the different positions. The position clearly has a effect on the measured temperature. Even during the exposure at  $t = 0$  s the temperature is dependent on the positioning.

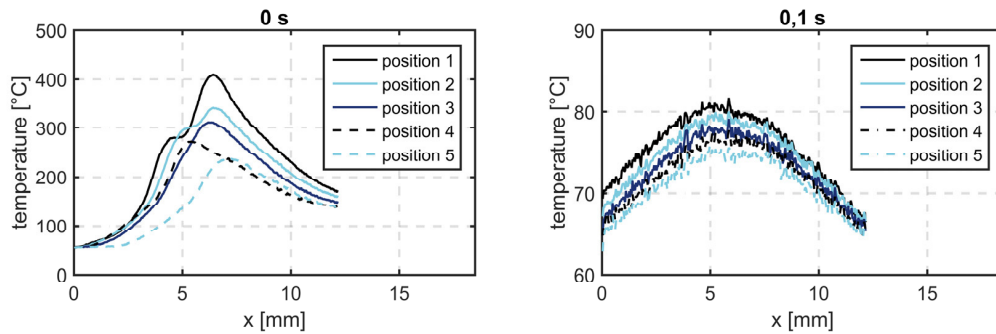
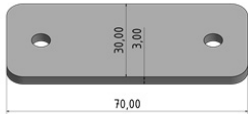
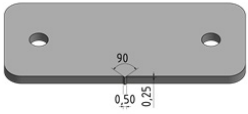
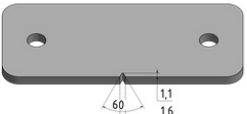
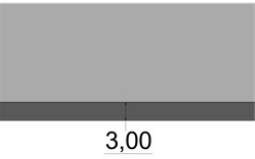
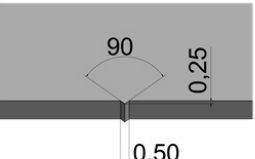
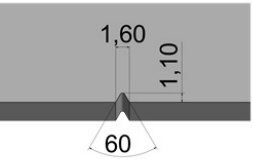
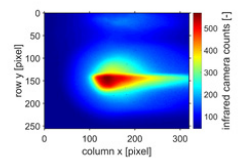
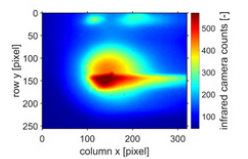
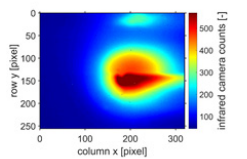



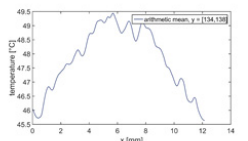
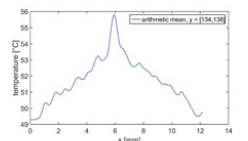
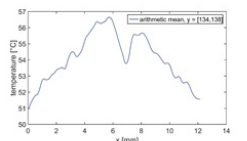


Fig. 6. Variation of the laser spot position on the specimen (a) temperatures measured at  $t = 0$  s, (b) temperatures measured at  $t = 0.1$  s.

#### 4.3. Flaws and their effects on the edge temperature

To investigate the influence of flaws, different flaws are simulated including mechanical and chemical flaws. The mechanical flaws have been investigated through notches and microjoints by means of the dimensions displayed in table 3. In comparison a flawless specimen is analyzed. The chemical flaws are supposed to simulate different impurities occurring in production. For example, remains of foil can be found at the edges of foiled sheet metals. They are simulated through strips of adhesive tape. Apart from paints also grease and oil can be found at the surface of the sheet metal parts. They are represented by WD-40® in the experiments.

Table 3. Influences of mechanical flaws on the quality assurance approach.

	Flawless specimen	Microjoint	Notch
Dimensions			
Dimensions			
IR-thermography			
Deburred edge			
Edge temperature			

The temperature curves of the defect experiments are compared to an optimal flawless temperature curve. The deviation of experimental temperatures to the flawless temperature curve indicate the existence of notches and microjoints (Fig. 7).

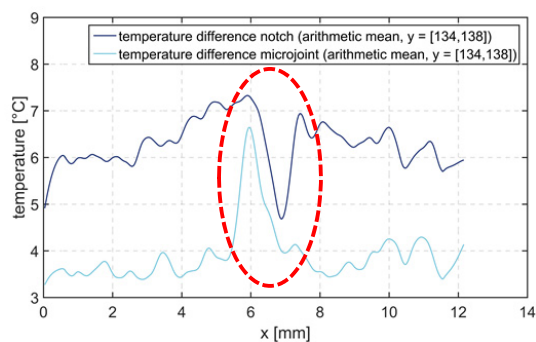
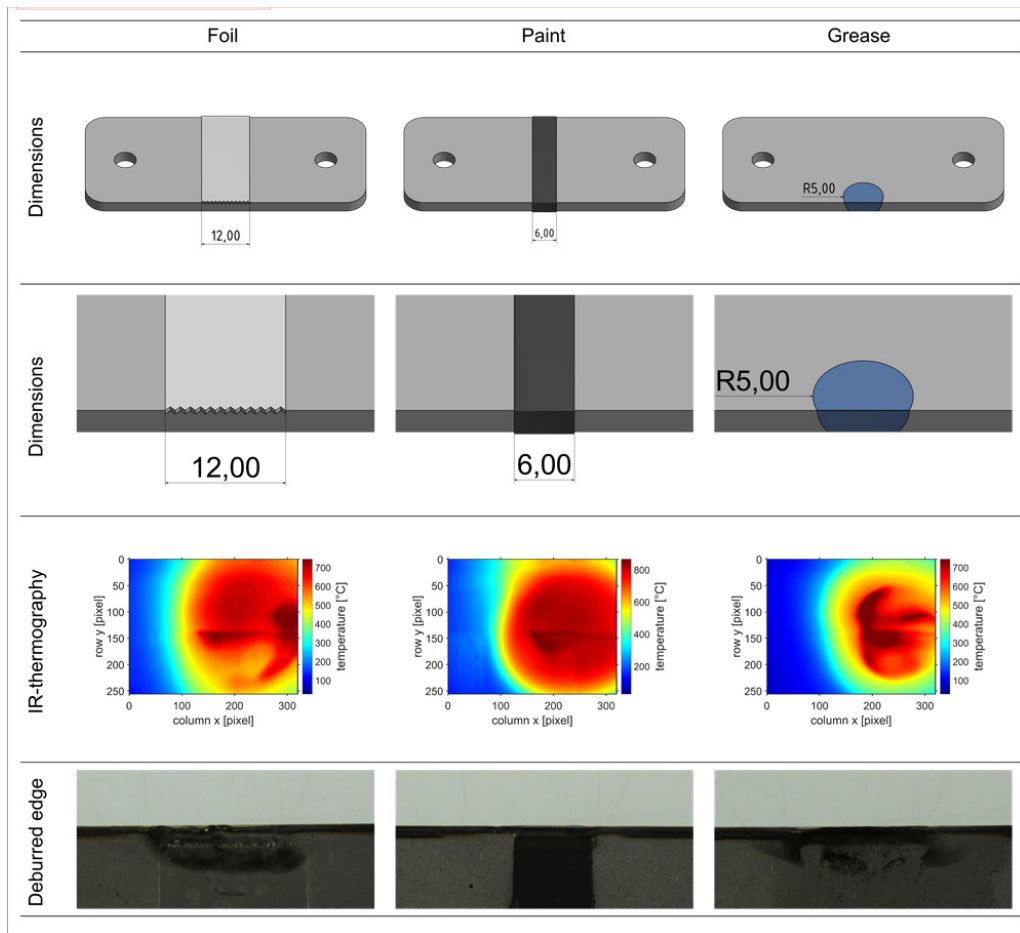


Fig. 7. Temperature curve measured in IR-thermography for notch.



Table 4. Influences of chemical flaws on the quality assurance approach.



The extensive temperature field (Tab. 4) caused by the combustion processes for the chemical flaws demonstrate the possibility to also reproducibly detect these flaws by IR-thermography.

## 5. Conclusion

It has been shown that the temperature of the edge has a dependency to curvature both in the laser deburring process and when cooling. Thus, it is possible to estimate the curvature through the thermography.

Furthermore, the positioning can be controlled through the temperature at the edge. For this purpose, the temperature field next to the melted edge needs to be considered.

Finally, it has been proven that different flaws have an influence on the temperature field of the deburred edge. The chemical flaws are characterized by the burning of different materials. This burning stands out in IR-measurements due to extreme variations in temperature and temperatures that are many times higher. Mechanical flaws can be specifically detected through interruptions of the regular temperature field at the edge.

The shown relationship between the temperature and the radii in laser deburring processes set the base for the development of a quality assurance. It has been pointed out that IR-thermography is capable of detecting different flaws occurring in the sheet metal manufacturing environment.

## References

- Aurich, J. C.; Dornfeld, D.; Arrazola, P. J.; Franke, V.; Leitz, L.; Min, S. (2009): Burrs—Analysis, control and removal. In: CIRP Annals - Manufacturing Technology 58 (2), S. 519–542. DOI: 10.1016/j.cirp.2009.09.004.
- Bagavathiappan, S.; Lahiri, B. B.; Saravanan, T.; Philip, John; Jayakumar, T. (2013): Infrared thermography for condition monitoring – A review. In: Infrared Physics & Technology 60, S. 35–55. DOI: 10.1016/j.infrared.2013.03.006.
- Barile, Claudia; Casavola, Caterina; Pappalettera, Giovanni; Pappalettere, Carmine (2016): Analysis of crack propagation in stainless steel by comparing acoustic emissions and infrared thermography data. In: Engineering Failure Analysis. DOI: 10.1016/j.engfailanal.2016.02.022.
- Beier, Hans-Michael (1999): Handbuch Entgrattechnik. Wegweiser zur Gratminimierung und Gratbeseitigung für Konstruktion und Fertigung. München: Hanser.
- Beier, Hans-Michael; Nothnagel, Reinhard (2015): Praxisbuch Entgrattechnik. Wegweiser zur Gratminimierung und Gratbeseitigung für Konstruktion und Fertigung. 2., überarbeitete und erweiterte Auflage. München: Hanser. Online verfügbar unter <http://dx.doi.org/10.3139/9783446444492>.
- Bernhard, Frank (2014): Handbuch der Technischen Temperaturmessung. Berlin, Heidelberg: Springer Berlin Heidelberg.
- Gillespie, LaRoux K. (2007): Mass finishing handbook. 1st ed. New York: Industrial Press.
- Krauss, Harald; Zeugner, Thomas; Zaeh, Michael F. (2014): Layerwise Monitoring of the Selective Laser Melting Process by Thermography. In: Physics Procedia 56, S. 64–71. DOI: 10.1016/j.phpro.2014.08.097.
- Lee, S. H. (2000): Analysis of Precision Deburring Using a Laser -An Experimental Study and FEM Simulation. In: KSME International Journal, S. 141–151.
- Purtonen, Tuomas; Kalliosaari, Anne; Salminen, Antti (2014): Monitoring and Adaptive Control of Laser Processes. In: Physics Procedia 56, S. 1218–1231. DOI: 10.1016/j.phpro.2014.08.038.
- Schäfer, Friedrich; Breuninger, Fritz (1975): Entgraten. Theorie, Verfahren, Anlagen. Mainz: Krausskopf (Buchreihe Produktionstechnik heute, 14).
- Schausberger, Florian; Speicher, Katrin; Steinboeck, Andreas; Jochum, Martin; Kugi, Andreas (2015): Two Illustrative Examples to Show the Potential of Thermography for Process Monitoring and Control in Hot Rolling. In: IFAC-PapersOnLine 48 (17), S. 48–53. DOI: 10.1016/j.ifacol.2015.10.076.
- Schmidt-Sandte, T. (2002): Laserstrahlbasierte Entgratverfahren für feinwerktechnische Anwendungen. Dissertation. Technischen Universität Carolo-Wilhelmina zu Braunschweig, Braunschweig. Fakultät für Maschinenbau und Elektrotechnik.
- Speka, Maryna; Mattei, Simone; Pilloz, Michel; Ilie, Mariana (2008): The infrared thermography control of the laser welding of amorphous polymers. In: NDT & E International 41 (3), S. 178–183. DOI: 10.1016/j.ndteint.2007.10.005.
- Spellenberg, Bernd; Zettner, Jürgen; Schreer, Oliver; Bassler, Michael; Haller, Manfred; Lenzi, Thomas; Hierl, Thomas: Inspection of laser-seam welds in automobile manufacturing, S. 388–398. DOI: 10.1117/12.603771.
- Thilow, Alfred P. (2008): Entgrattechnik. Entwicklungsstand und Problemlösungen. 3., verb. Aufl. Renningen: expert-Verl. (Kontakt & Studium, 392).
- Usamentiaga, Rubén; Venegas, Pablo; Guerediaga, Jon; Vega, Laura; Molleda, Julio; Bulnes, Francisco (2014): Infrared Thermography for Temperature Measurement and Non-Destructive Testing. In: Sensors 14 (7), S. 12305–12348. DOI: 10.3390/s140712305.